Equilibrium, multistability, and chiral asymmetry in rotated mirror plasmas

P. M. Valanju[a] and S. M. Mahajan
Institute for Fusion Studies, The University of Texas at Austin, Austin, Texas 78712-1060

H. J. Quevedo
Fusion Research Center, The University of Texas at Austin, Austin, Texas 78712-1060

(Received 3 April 2006; accepted 10 May 2006; published online 14 June 2006)

The Hall term in two-fluid magnetohydrodynamics is shown to be necessary to balance the curl of the ion inertial force in a rotating plasma with spatially nonuniform crossed electric and magnetic fields. Two-fluid solutions are obtained that qualitatively explain the multistable rotational response observed in magneto-Bernoulli experiment, imply chiral symmetry breaking, i.e., handedness, and yield new dynamo-like electromotive terms in the effective circuit equation for externally rotated mirror plasma equilibria. © *2006 American Institute of Physics*. [DOI: 10.1063/1.2209967]

I. INTRODUCTION

Multistable rotational plasma response is observed in many open-ended machines.[1–3] In the magneto-Bernoulli experiment (MBX) (Fig. 1), we observe fast, spontaneous jumps (similar to L-H transitions) between different near-sonic plasma rotation equilibria whereas the externally applied voltages are kept fixed (Fig. 2). We will show that (1) the $\mathbf{j}\times\mathbf{B}$ Hall term in the electron momentum equation cannot be neglected, i.e., two-fluid theory must be used, when the ion inertial force density $\mathbf{F}\equiv nm_i\mathbf{V}\cdot\nabla\mathbf{V}$ has nonzero curl, (2) as the inertial centrifugal force always points radially outward independent of the rotation direction (Fig. 3), chiral symmetry, i.e., handedness or symmetry under reflection, is broken, (3) two-fluid solutions qualitatively explain the multistable rotational response observed in MBX (Fig. 4), (4) the coupling between electromagnetic and inertial forces yields a dynamo-like integral circuit equation with a new electromotive voltage term proportional to the angular velocity and the net current (Fig. 5), and (5) the chiral asymmetry, multistability, and the dynamo-like behavior are related—their microscopic origin is the large difference between ion and electron masses $m_i \gg m_e$.

II. MBX ROTATING MIRROR DEVICE

We begin with a brief description of the MBX device and relevant observations. In MBX (Fig. 1), two sets of 0.3 m radius circular mirror coils 1 m apart create a magnetic field of 400 G at the midplane ($z=0$) with a mirror ratio of 7.4. The low density ($n_i \sim 5\times10^{15}/\mathrm{m}^3$) hydrogen target plasma is rotated to Mach$\sim$1 by biasing, up to 300 V, two equal-area ring electrodes mounted on a ceramic insulator near one end of the mirror. A grounded limiter ring provides the return current path (Fig. 3). The applied voltages, the current drawn by each end ring electrode, the gas fill pressure ($\sim$0.2 m Torr), and the net electron-cyclotron power ($\sim$800 W) are the global measurements. The angular rotation profile $\Omega(\mathbf{r})$ is measured by a movable Mach probe at $z=0$. A movable Langmuir probe at $z=0$ and three fixed Langmuir probes near $z=L$ measure plasma potential $\Phi(\mathbf{r})$. The voltage between the probes at $z=L$ and the ring electrodes gives the drop Φ_s across the sheath. The plasma rotation penetration to the center plane shows a unipolar, multistable response to external voltages applied at electrode rings at the mirror end. When the electrode rings are biased positive with respect to the limiter, more current is drawn (Fig. 2) from the end rings, the radial electric field $\mathbf{E}(\mathbf{r})$ penetrates better to the center ($z=0$) and the angular rotation speed $\Omega(r,z=0)$ is faster. At Mach numbers $(V/V_{\mathrm{th}})\geq 1$, i.e., at voltages above +120 V between the innermost ring and the limiter (Fig. 2), we observe fast, spontaneous bifurcations, with hysteresis, between two or three discrete, long-lived ($\sim$20 ms) equilibrium rotation profiles (Fig. 2). More experimental details will be presented in another article.

III. MBX ROTATING MIRROR THEORY

To construct a self-consistent theory of such externally rotated, multistable equilibria, we start with the two-fluid (Hall) magnetohydrodynamic (MHD) electron and ion force equations

$$e[\mathbf{E}+\mathbf{V}\times\mathbf{B}]=\mathbf{j}\times\mathbf{B}/n-\nabla\cdot\bar{P}_e/n+\mathbf{f}_e, \tag{1}$$

$$m_i[\partial_t\mathbf{V}+\mathbf{V}\cdot\nabla\mathbf{V}]=e[\mathbf{E}+\mathbf{V}\times\mathbf{B}]-\nabla\cdot\bar{P}_i/n+\mathbf{f}_i, \tag{2}$$

where $\mathbf{f}_e=e\eta\mathbf{j}$ and $\mathbf{f}_i=-\gamma m_i\mathbf{V}-\mathbf{f}_e$. We set electron mass $m_e\approx 0$, so that $\mathbf{V}_i=\mathbf{V}$, $\mathbf{V}_e=\mathbf{V}-\mathbf{j}/en$. The total pressure tensor is $\bar{P}=\bar{P}_i+\bar{P}_e=p\bar{I}+\bar{\Pi}$, with scalar p, unit tensor $\bar{I}$, and $\nabla\cdot\bar{\Pi}\approx-\mu_e\nabla^2\mathbf{V}_e-\mu_i\nabla^2\mathbf{V}_i$. The resistivity η, the ion-neutral charge-exchange frequency γ, and the viscosities μ_e and μ_i are all small but not exactly zero in MBX. Hence $\nabla\cdot\bar{P}\approx\nabla p$. All dissipative mean free paths are of order many meters in MBX whose $R=0.25$ m.

We assume constant density n. Using n, the average B_0, R at $z=0$, and the average sound speed V_0 as units, so that

[a]E-mail: pvalanju@mail.utexas.edu

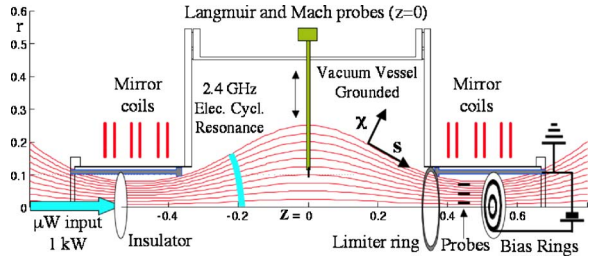

FIG. 1. Schematic of MBX rotating mirror device.

$$\mathbf{B} = B_0\hat{\mathbf{B}}, \quad \mathbf{V} = V_0\hat{\mathbf{V}}, \quad \mathbf{r} = R\hat{\mathbf{r}}, \quad t = (R/V_0)\hat{t},$$

$$\mathbf{E} = V_0B_0\hat{\mathbf{E}}, \quad \mathbf{j} = (enV_0)\hat{\mathbf{j}}, \quad p_{e,i} = (nm_iV_0^2)\hat{p}_{e,i}, \tag{3}$$

$$\hat{\eta} = \nu_{ei}/\Omega_e, \quad \gamma = (V_0/R)\hat{\gamma},$$

and Eqs. (1) and (2) are cast into the dimensionless form[4]

$$\hat{\mathbf{E}} + (\hat{\mathbf{V}} - \hat{\mathbf{j}}) \times \hat{\mathbf{B}} = \hat{\eta}\hat{\mathbf{j}} - \epsilon\hat{\nabla}\hat{p}_e, \tag{4}$$

$$\hat{\mathbf{E}} + \hat{\mathbf{V}} \times (\hat{\mathbf{B}} + \epsilon\hat{\nabla} \times \hat{\mathbf{V}}) = \epsilon[\hat{\partial}_t\hat{\mathbf{V}} + \hat{\nabla}\hat{p}_i + \hat{\nabla}\hat{V}^2/2] + \hat{\gamma}\hat{\mathbf{V}} + \hat{\eta}\hat{\mathbf{j}}, \tag{5}$$

where $\epsilon \equiv (\lambda_i/R)(V_0/V_A) \approx 0.025$ in MBX, $V_A = B_0/\sqrt{\mu_0 m_i n}$ is the Alfvén speed, $\lambda_i = \sqrt{m_i/\mu_0 ne^2} = V_A/\omega_{ci}$ is the ion skin depth, ν_{ei} is the electron-ion collision frequency, and Ω_e is the electron gyrofrequency.

We will use normalized fields but drop all hats, and set η and γ negligibly small. The net (ion+electron) force equation is

$$\mathbf{j} \times \mathbf{B} = \epsilon[\nabla(P + V^2/2) + (\nabla \times \mathbf{V}) \times \mathbf{V} + \gamma\mathbf{V}]. \tag{6}$$

At small r, the normalized axisymmetric external vacuum field $\mathbf{B}_0$ of mirror ratio $R_M = (1+q)/(1-q)$ is

$$\mathbf{B}_0 = \nabla\Psi_0 \times \frac{\hat{\theta}}{r}, \quad \Psi_0 = \frac{r^2}{2} - \frac{qr}{k}I_1(kr)\cos(kz), \tag{7}$$

where I_1 is a Bessel function.

The $\mathbf{j}\times\mathbf{B}$ Hall term in Eq. (4) and the $\mathbf{V}\times(\nabla\times\mathbf{V})$ inertial term in Eq. (5) contain solenoidal forces, i.e., forces with nonzero curl so that $\int_s \nabla\times\mathbf{F} = \oint d\mathbf{l}\cdot\mathbf{F} \neq 0$. *These internal torques cannot be balanced by any curl-free gradient forces*. Solenoidal and gradient forces must be balanced separately to obtain a long-lived equilibrium.

For example, consider the "isorotating" state in which the angular speed is constant along each $\mathbf{B}$ field line, i.e., $\Omega = \Omega(\Psi_0)$. If the magnitude of $\mathbf{B}_0$ varies along field lines (as in the mirror), the curl of the centrifugal force $F_c \sim V_\theta^2/r$, which is a part of the inertial force $\mathbf{V}\times(\nabla\times\mathbf{V})$, is not zero but is proportional to $\partial_z\Omega^2$ (see Fig. 3). It must be balanced by the curl of $\mathbf{j}\times\mathbf{B}$. At near-sonic V_θ, $\mathbf{F}_c$ is comparable to ∇p and its curl is large. The current $\mathbf{j} = \mathbf{j}_c + \mathbf{j}_d$ contains two comparable parts: $\mathbf{j}_c$ balances the curly part of $\mathbf{F}_c$ whereas the "diamagnetic current" $\mathbf{j}_d$ balances curl-free gradient forces in Eq. (6). MBX was specifically designed to explore the effects of solenoidal forces at high rotation speeds in nonuniform $\mathbf{B}$.

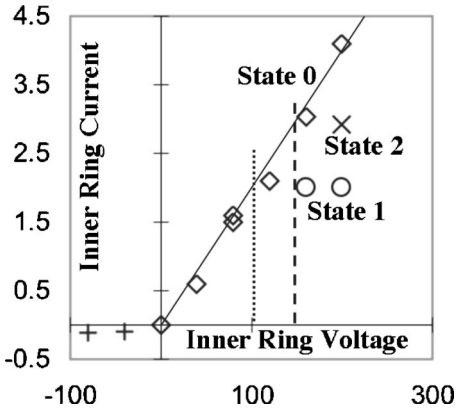

FIG. 2. Multiple distinct states (two above +110 V and three above +150 V) in MBX. The plasma spontaneously jumps between these states. The current near zero voltage agrees with electrode area and $I-V$ characteristics at the plasma density.

Solenoidal forces can be isolated by annihilating all gradient forces with curl. Eqs. (4) and (5) become strong curl balance conditions that *must* be satisfied by all equilibria. In the dissipationless limit $\eta \approx 0$, $\gamma \approx 0$, $\mu_{e,i} \approx 0$, they are

$$\nabla \times [\mathbf{V}_e \times \mathbf{B}] = \nabla \times [(\mathbf{V} - \mathbf{j}) \times \mathbf{B}] = 0, \tag{8}$$

$$\nabla \times [\mathbf{B}_i \times \mathbf{V}] = \nabla \times [(\mathbf{B} + \epsilon\nabla \times \mathbf{V}) \times \mathbf{V}] = 0. \tag{9}$$

Thus, in Hall MHD, $\mathbf{B}$ guides the electron flow but an effective field $\mathbf{B}_i = \mathbf{B} + \epsilon\nabla\times\mathbf{V}$ guides the ion flow $\mathbf{V}$. The following curls are equal, but they need not be zero

$$\nabla \times [\mathbf{V} \times \mathbf{B}] = \nabla \times [\mathbf{j} \times \mathbf{B}] = \epsilon\nabla \times [(\nabla \times \mathbf{V}) \times \mathbf{V}]. \tag{10}$$

In single-fluid MHD,[5–8] the $\mathbf{j}\times\mathbf{B}$ Hall term is dropped in the electron Eq. (8). Hence, *all three terms in* Eq. (10) *must be separately zero in single-fluid MHD*, making it too restrictive to accurately model sheared flows. For example, the familiar isorotating[9] MHD flow

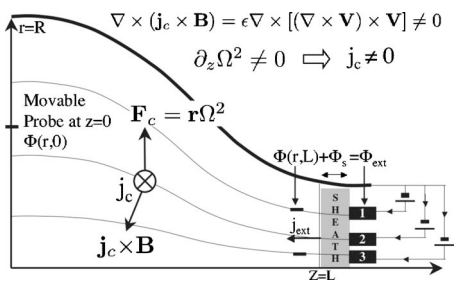

FIG. 3. The inertial force $\mathbf{F}_c$ inevitably varies with z in a mirror. At sonic speeds, $\mathbf{F}_c$ has a large nonzero $\nabla\times\mathbf{F}_c$ that must be balanced in the net momentum equation with $\nabla\times(\mathbf{j}_c\times\mathbf{B})$. Two-fluid (Hall) theory is thus essential to calculate $\mathbf{j}_c$.

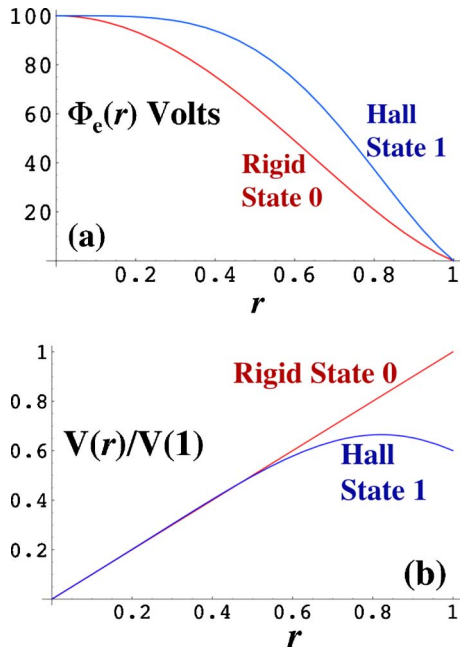

FIG. 4. (a) Electric potential Φ_e [see Eq. (19)] and (b) rotation speed vs r for rigid rotation with globally constant $\Omega=\omega_0$, and for the Hall solution of Eq. (16) with parameters chosen to get the same potentials at $r=0$ and $r=1$. Rigid rotation is faster than the Hall solution. We identify them with State 0 and State 1 of Fig. 2 respectively.

$$\mathbf{V}=\mathbf{V}_0=\mathbf{E}\times\mathbf{B}/B^2=r\Omega(\Psi)\hat{\theta},\quad \mathbf{B}\cdot\nabla\Psi=0, \tag{11}$$

does not satisfy Eq. (10) in the collisionless limit unless Ω is globally constant because $\nabla\times[\mathbf{V}\times(\nabla\times\mathbf{V})]=\partial_z(r\Omega^2)\hat{\theta}\neq 0$ when $\partial_z B\neq 0$. Single fluid MHD cannot consistently balance the nonzero curl of the centrifugal inertial force $F_c=r\Omega^2$ when $\partial_z F_c=0$. Even for a nonisorotating $\Omega(r)$ with $\partial_z F_c=0$, the MHD curl problem just shifts to $\nabla\times[\mathbf{V}\times\mathbf{B}]=[\partial_z\Omega\partial_r\Psi-\partial_r\Omega\partial_z\Psi]\hat{\theta}\neq 0$ in Eq. (10). The only isorotating MHD solution in which all curls in Eq. (10) are zero is the shear-free, globally rigid rotation $\Omega(\mathbf{r})=\Omega_0$.

In contrast, two-fluid Hall MHD can have sheared flows in which $\nabla\times[\mathbf{V}\times\mathbf{B}]$, $\nabla\times[\mathbf{j}\times\mathbf{B}]$, and $\nabla\times[\mathbf{V}\times(\nabla\times\mathbf{V})]$ in Eq. (10) are all nonzero but balance each other. A solution of Eq. (8) (and Eq. (4) with η set to 0) is one where electrons isorotate under an effective field $\mathbf{E}_e=-\nabla\Phi_e\equiv-\nabla(\Phi-\epsilon p_e)$ and the net $\mathbf{B}$, i.e., $\mathbf{V}_e=\mathbf{V}_0=\mathbf{E}_e\times\mathbf{B}/B^2$. To balance $\partial_z(r\Omega^2)\hat{\theta}$ in Eq. (9), we let the ion and electron flows differ by $\mathbf{v}=\mathbf{j}\neq\mathbf{0}$:

$$\mathbf{V}=\mathbf{V}_0+\mathbf{v},\quad \mathbf{V}_0=\mathbf{E}_e\times\mathbf{B}/B^2,\quad \mathbf{v}=\mathbf{j}=\epsilon\nabla\times\mathbf{b}/M_A^2,$$
$$\mathbf{B}=\mathbf{B}_0+\mathbf{b},\quad \nabla\times\mathbf{B}_0=0,\quad \nabla\times(\mathbf{V}_0\times\mathbf{B})=0. \tag{12}$$

Assuming $\mathbf{j}=r\omega\hat{\theta}$, the second part of Eq. (10) becomes

$$\nabla\Psi\times\nabla\omega=\frac{\epsilon}{2}\nabla(\Omega_0+\omega)^2\times\nabla r^2=\epsilon r\partial_z[\Omega_0+\omega]^2\hat{\theta}. \tag{13}$$

For $|\mathbf{j}|\ll|\mathbf{V}_0|$ $(\omega\ll\Omega_0)$, and $|\mathbf{b}|\ll|\mathbf{B}_0|$ $(\Psi\sim\Psi_0)$,

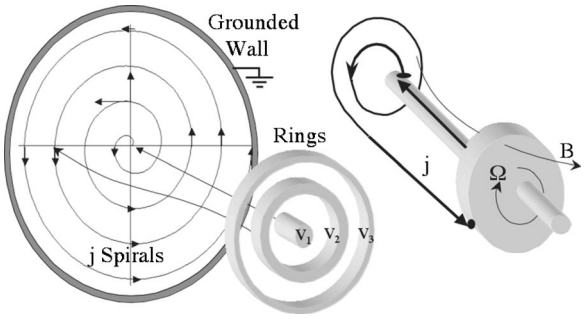

FIG. 5. Electromagnetic and inertial forces together yield a spiral flow pattern of current **J** lines that resembles Fig. 1 of Ref. 10 (as shown on the right-hand side), leading to a dynamo-like integral circuit equation with a new, nonresistive term $\mathcal{M}\Omega I$. The difference between ion and electron masses breaks the chiral symmetry, giving the spiral current paths of unique helicity that are needed for such a dynamo to work.

$$\nabla\Psi_0\times\nabla\omega=\frac{\epsilon}{2}\nabla[\Omega_0(\Psi_0)]^2\times\nabla r^2$$
$$=\frac{\epsilon}{2}\frac{d\Omega_0^2}{d\Psi_0}\nabla\Psi_0\times\nabla r^2$$
$$=\frac{\epsilon}{2}\nabla\Psi_0\times\nabla\left(r^2\frac{d\Omega_0^2}{d\Psi_0}\right). \tag{14}$$

This equation has solutions of the form

$$\omega=\epsilon r^2\Omega_0(\Psi_0)\frac{d\Omega_0(\Psi_0)}{d\Psi_0}+F(\Psi_0), \tag{15}$$

where F is an arbitrary function. If $\Omega_0(\Psi_0)$ and $F(\Psi_0)$ are constants, ions and electrons rotate rigidly at slightly different speeds so the current is small but nonzero. For an isorotating plasma where $\Omega_0(\Psi_0)$ is not constant, one possible solution is

$$\Omega_0(\Psi_0)=\omega_0\Psi_0,\quad F(\Psi_0)=\omega_f \tag{16}$$

with constants ω_f and ω_0, and Ψ_0 given by Eq. (7). Thus

$$V_\theta(r,z)=r\Omega,\quad \Omega=\omega_0\Psi_0+\omega_f+\epsilon r^2\omega_0^2\Psi_0, \tag{17}$$

$$v_\theta(r,z)=j_\theta=r\omega,\quad \omega=\omega_f+\epsilon r^2\omega_0^2\Psi_0. \tag{18}$$

Thus, unlike single-fluid MHD, two-fluid MHD has solutions for which the curls in Eq. (10) are all nonzero but balance each other in a self-consistent fashion.

When $b\ll B_0$, the electric field consistent with the rotation profile is set by the electron force equation

$$\mathbf{E}_e=-\nabla\Phi_e=-\nabla(\Phi-\epsilon p_e)\approx\mathbf{B}_0\times\mathbf{V}_0$$
$$=-\Omega_0(\Psi_0)\nabla\Psi_0. \tag{19}$$

Electric potentials and rotation speeds for rigid rotation $\Omega_0(\Psi_0)=\omega_0$ and for the two-fluid (Hall) solution $\Omega_0(\Psi_0)=\omega_0\Psi_0$ of Eq. (16) are $\Phi_{e,\mathrm{RR}}=\omega_0\Psi_0$ and $\Phi_{e,\mathrm{Hall}}=\omega_0\Psi_0^2/2$, respectively. They are shown in Fig. 4.

To derive a "circuit equation," we use $\nabla\cdot\mathbf{j}=0$ along with V_θ, j_θ from Eqs. (17) and (18) in the lowest order θ component of Eq. (6) (balance between the externally applied torque and the charge-exchange drag on neutrals)

$$j_z B_r - j_r B_z = \gamma V_\theta, \quad \partial_r j_r + \partial_z j_z = 0. \tag{20}$$

This relates (j_r, j_z) to V_θ, j_θ for small but nonzero dissipation. The currents drawn are thus proportional to the rotation speed. The ordering we used is valid for small γ because very small (j_r, j_z) can drive large near-sonic V_θ.

The plasma is in series with the sheath in the rotation-driving circuit, so the externally applied ring voltage is dropped across the sheath and the plasma: $\Phi_{\text{ext}}(r) = \Phi_s + \Phi(r, L)$. For a given $\Phi_{\text{ext}}(r)$, the potential drop Φ_s across the thin ($\sim 10^{-4}$ m) sheath and the current $j_z(r, L)$ flowing through the sheath must satisfy the standard sheath $I-V$ characteristic for the ring electrode. This boundary condition gives the "circuit equation" for the net current $I(r)$ and rotation $\Omega(\Psi)$ driven by applying external voltage $\Phi_{\text{ext}}(r)$ to the magnetic surface labeled by $\Psi(r, L)$,

$$\Phi_{ext}(r) = \Phi_s + \mathcal{E}(\Psi) + \mathcal{R}(\Psi) I(r) + \frac{\int I dt}{C(\Psi)} + \mathcal{L}(\Psi)\frac{dI}{dt}, \tag{21}$$

$$\mathcal{E}(\Psi) = \mathcal{M}(\Psi)\Omega(\Psi) I(\Psi) + \mathcal{K}(\Psi) I^2(\Psi) + \cdots. \tag{22}$$

For a given rotation profile and η and γ, this is derived by integrating Eq. (19) for the potential drop, and using Eq. (20) for the current in the $r-z$ plane. The sheath drop Φ_s is small $\sim T_e$. The plasma resistance, inductance, capacitance ($\mathcal{R}$, $\mathcal{L}$, and $\mathcal{C}$) and the new $\mathcal{M}$, $\mathcal{K}$ depend on the geometry and the $\Omega(\Psi)$ profile. $\mathcal{E}$ is necessary for consistency. It arises in two-fluid Hall MHD which provides an intrinsic plasma length scale λ_i.

The fastest solution is the rigid rotation (constant Ω) as shown in Fig. 4. According to Eq. (20), it draws the maximum current (j_r, j_z) for a given applied voltage. Also, the two-fluid $\mathcal{M}\Omega I$ effects are absent in rigid rotation, so the voltage $\mathcal{R}I$ varies linearly with I. Hence we identify rigid rotation with the "State 0" and the slower Hall-MHD V_θ of Eq. (17) with "State 1" in Fig. 2. As the inertial force is nonlinear in V_θ, more states like "State 2" can occur for a given voltage applied on the end ring. All these states asymptote to the rigid rotator near $r=0$.

The circuit equation is similar to the homopolar disk dynamo Eq. (1.1) of Ref. 10, hence we use $\mathcal{M}$ to label the term proportional to I. The steady-state electromotive force (EMF $\mathcal{E}$) is the reaction to the mechanical torque that *must* be supplied, even for a time-independent rotation, to balance the curl of the inertial (centrifugal) force arising from the inevitable z variation of Ω—as in a mirror. Its magnitude does not vanish in the small but finite dissipation limit. The rotating plasma constantly tries to "straighten" the **B** field by generating the j_θ in Eq. (18), separating ions from electrons isorotating in **B**.

The inertial centrifugal force $\mathbf{F}_c$ is always radially outward independent of the rotation direction. Hence the curl-balancing $\mathbf{j}_c$ does not change sign with **E** (or $j_\perp$). As shown in Fig. 5, j_θ is always in one direction independent of the direction of $j_\perp$, which changes with $E_\perp$; the current paths in two-fluid plasma have the unique handedness (chirality) that is necessary for generating $\mathcal{E}$.

Unlike single-fluid MHD, solutions with opposite signs of $\zeta \equiv \mathbf{E}\cdot\mathbf{j}\times\mathbf{B}$ are not equivalent in Hall-MHD. Ions rotate faster or slower than electrons depending on the sign of ζ. The unidirectionality of inertial centrifugal force implies chiral symmetry breaking; right- and left-handed rotations (with respect to **B**) are not equivalent. The spiral current paths have unique chirality (handedness) in two-fluid MHD, and the resulting inertial EMF $\mathcal{E}$ is the macroscopic manifestation of the chiral symmetry breaking. States with such spiral currents are two-fluid states that rotate slower than the "rigid rotator" MHD state which has no velocity shear and $j_\theta = 0$. The observation of the low-rotation "State 1", and its deviation from the linear $\Phi = \mathcal{R}\mathcal{I}$ relation for the high-rotation "State 0," is direct experimental proof of chiral symmetry breaking.

The microscopic cause of the chiral symmetry breaking in equilibrium is that the handedness of the heavy ions and light electrons rotating around the magnetic field is opposite, and their mass difference forces them to move separately. Electrons stay more closely tied to **B**, keeping $E_\parallel = 0$ along the net **B**. Ions dominate the net flow, which must differ from isorotating MHD flow $\mathbf{E}\times\mathbf{B}$ when inertial forces are big and **B** varies in space.

We have not addressed the stability of these states or the spontaneous transitions between them observed in MBX. That requires time-dependent numerical calculations. We have focused here on extracting only the chiral symmetry information in a simple form. Time dependence and stability will be addressed in a later article.

The linear approximation we have used for near-sonic rotation speeds becomes inadequate for higher, near-Alfvén rotation speeds. The effect of the diamagnetic self-field may become large enough to support internal states with field lines detached from the ends. Before resorting to numerical solutions, one can find special sets of analytic solutions of the nonlinear Eqs. (8) and (9) by using the linearizing "double Beltrami" ansatz

$$\mathbf{v}_e \equiv \mathbf{v} - \epsilon \nabla \times \mathbf{b}/M_A^2 = a_e \mathbf{b}, \quad \mathbf{b}_i \equiv \mathbf{b} + \epsilon \nabla \times \mathbf{v} = a_i \mathbf{v}, \tag{23}$$

where a_e and a_i are real constants. This yields a multitude of interesting exact solutions. One can use the same procedure as shown here to match these solutions to the external circuit, and in that process, reject some solutions for being incompatible with the boundary conditions. However, as MBX has reached near-sonic but not near-Alfvén speeds so far, we will present such solutions in a subsequent article.

ACKNOWLEDGMENTS

The basic ideas in this work were presented in an APS-DPP invited talk (Ref. 2) in November 2003.

The authors gratefully acknowledge support from R. Hörlein, R. D. Bengtson, J.C. Wiley, and K. Carter, from the US-DOE, ICC Grant No. DOE-FG02-03ER54697, and an IFS Grant.

[1] S. Shinohara and S. Matsuyama, Phys. Plasmas **9**, 4540 (2002).
[2] P. M. Valanju, Bull. Am. Phys. Soc. **48**, 168 (2003).
[3] R. F. Ellis, A. B. Hassam, S. Messer, and B. R. Osborn, Phys. Plasmas **8**, 2057 (2001); R. F. Ellis, A. Case, R. Elton, J. Ghosh, H. Griem, A. Hassam, R. Lunsford, S. Messer, and C. Teodorescu, *ibid.* **12**, 055704 (2005).
[4] S. M. Mahajan and Z. Yoshida, Phys. Rev. Lett. **81**, 4863 (1998); Phys. Plasmas **7**, 635 (2000); Phys. Rev. Lett. **88**, 095001 (2002).
[5] A. Y. Aydemir, Phys. Plasmas **11**, 5065 (2004).
[6] A. B. Hassam, Phys. Plasmas **6**, 3738 (1999).
[7] L. C. Steinhauer, Phys. Fluids **24**, 328 (1981).
[8] A. V. Turlapov and V. E. Semenov, Phys. Rev. E **57**, 5937 (1998).
[9] B. Lehnert, Nucl. Fusion **11**, 485 (1971).
[10] H. K. Moffatt, *Magnetic Field Generation in Electrically Conducting Fluids* (Cambridge University Press, Cambridge, 1978), p. 3.